

Structural Phase Transitions in BaTiO₃ Studied via Perturbed Angular Correlations

J. Roth, M. Uhrmacher, P. de la Presa, L. Ziegeler, and K. P. Lieb

II. Physikalisches Institut, Bunsenstr. 7 - 9, Universität Göttingen, D-37073 Göttingen

Reprint requests to Dr. M. U.; Fax: +49-551-394493; E-mail: uhrmacher@up2u06.gwdg.de

Z. Naturforsch. **55 a**, 242–246 (2000); received August 24, 1999

Presented at the XVth International Symposium on Nuclear Quadrupole Interactions, Leipzig, Germany, July 25 - 30, 1999.

Phase transitions in the ferroelectric perovskite BaTiO₃ were studied for ¹¹¹In-implanted polycrystalline samples by measuring the electric field gradients by means of Perturbed Angular Correlation spectroscopy. The phase transitions between the orthorhombic ⇌ rhombohedral ⇌ tetragonal ⇌ cubic lattices were investigated in 2 - 10 K steps, for increasing and decreasing temperatures, in order to determine their hysteresis. The transition parameters are compared with results from measurements of the spontaneous polarization, electric susceptibility and neutron scattering.

Key words: Perturbed Angular Correlations; BaTiO₃; Phase Transitions; Hysteresis; ¹¹¹In.

1. Introduction

Among the perovskites, BaTiO₃ is the most important ferroelectric compound which is widely used in electromechanical actuators, sensors, ceramic capacitor dielectrics and photo-galvanic devices [1-3]. Its crystal structures, structural and electric phase transitions have been analyzed in much detail using several methods, such as neutron and X-ray diffraction, electric susceptibility, etc. Previous results from Perturbed Angular Correlation (PAC) spectroscopy in BaTiO₃, Ba(TiHf)O₃, and CdTiO₃ using ¹⁸¹Hf/¹⁸¹Ta probes have been reported by Catchen et al. [4 - 6] and by Schäfer et al. [7]. Recently, Uhrmacher and collaborators [8] have published first PAC results in BaTiO₃ using ¹¹¹In/¹¹¹Cd hyperfine probes. Their survey measurements showed the occurrence of electric field gradients (EFG) in the non-cubic phases, present below the Curie temperature $T_C = 393$ K. Structural phase transitions can be monitored via PAC, if the hyperfine probe atoms substitute specific cation lattice sites. Several recent studies on perovskites of the type A²⁺B⁴⁺O₃ [9, 10] using ¹⁸¹Hf and ¹¹¹In probe nuclei have given evidence that the main hyperfine fraction can be attributed to substitutional B-site implantation of the probes.

The present PAC measurements for ¹¹¹In/¹¹¹Cd probes in polycrystalline BaTiO₃ samples aim at scan-

ning, in finer temperature steps than in [8], the structural phase transitions, which occur between the cubic phase (I, paraelectric), the tetragonal phase (II), the orthorhombic phase (III), and the rhombohedral phase (IV). The approximate transition temperatures are $T_0 = 193$ K for the IV ⇌ III transition, $T_0' = 278$ K for the III ⇌ II transition and $T_C = 393$ K for the II ⇌ I transition [4 - 6, 8].

2. Experiments

The PAC measurements were carried out for polycrystalline BaTiO₃ powder samples of 99.995% purity which were pressed into pellets, 4 mm in diameter and 0.5 mm thick. Powder X-ray diffraction analyses at room temperature revealed that all observed reflexes could be assigned to the expected tetragonal phase. Some 10¹² ¹¹¹In⁺ ions were implanted at 400 keV ion energy into the samples, using the Göttingen ion implanter IONAS [11]; the implantation depth was about 60 nm. After implantation the samples were annealed for four hours at 1673 K in air in order to remove radiation damage. For the measuring temperatures below 300 K, the samples were mounted at the pole tip of either a closed-cycle helium cryostat ($T = 10 - 230$ K) or a Peltier element ($T = 275 - 296$ K). Both cryostates were housed in vacuum chambers at pressures of 10⁻⁶ - 10⁻⁵ mbar. Measurements above room temperature

0932-0784 / 00 / 0100-0242 \$ 06.00 © Verlag der Zeitschrift für Naturforschung, Tübingen · www.znaturforsch.com



Dieses Werk wurde im Jahr 2013 vom Verlag Zeitschrift für Naturforschung in Zusammenarbeit mit der Max-Planck-Gesellschaft zur Förderung der Wissenschaften e.V. digitalisiert und unter folgender Lizenz veröffentlicht: Creative Commons Namensnennung-Keine Bearbeitung 3.0 Deutschland Lizenz.

Zum 01.01.2015 ist eine Anpassung der Lizenzbedingungen (Entfall der Creative Commons Lizenzbedingung „Keine Bearbeitung“) beabsichtigt, um eine Nachnutzung auch im Rahmen zukünftiger wissenschaftlicher Nutzungsformen zu ermöglichen.

This work has been digitalized and published in 2013 by Verlag Zeitschrift für Naturforschung in cooperation with the Max Planck Society for the Advancement of Science under a Creative Commons Attribution-NoDerivs 3.0 Germany License.

On 01.01.2015 it is planned to change the License Conditions (the removal of the Creative Commons License condition "no derivative works"). This is to allow reuse in the area of future scientific usage.

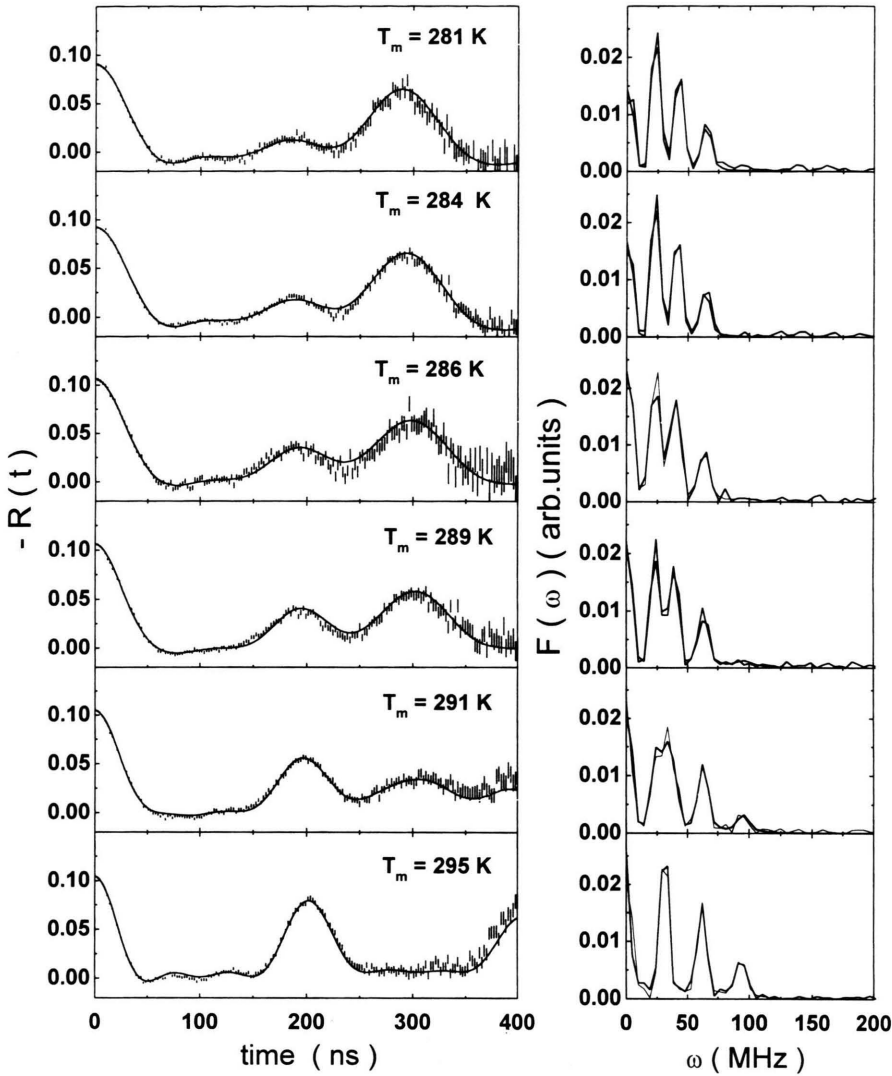


Fig. 1. Perturbation functions $R(t)$ and Fourier transforms $F(\omega)$ measured across the III \rightarrow II phase transition.

were carried out under air in an oven of low γ -ray absorption. We estimate that the given temperatures are correct within better than ± 0.4 K.

The PAC spectra were accumulated using a set-up of four NaI(Tl) detectors in 90° geometry. The perturbation functions $R(t)$ were fitted by assuming, at each temperature, two fractions f_i and $f_k = 1 - f_i$, which are characterized by their respective static EFG parameters [12], i. e. the quadrupole frequency ν_Q , asymmetry parameter η and frequency width δ . Figure 1 illustrates the evolution of the perturbation function $R(t)$ and its Fourier transform $F(\omega)$ across the III \Rightarrow II phase transition, where the temperature was increased from 281 K to 295 K. Evidently, as

shown in Fig. 2, the hysteresis of this phase transition shows up via the temperature dependences of the two competing fractions $f_{\text{III}}^{1/4}$ and $f_{\text{II}}^{1/4} = 1 - f_{\text{III}}^{1/4}$, for increasing or decreasing temperature. Finally, Fig. 3 displays the II \Rightarrow I phase transition which occurs very suddenly.

3. Electric Field Gradients and Site Occupation

The deduced EFG parameters for ^{111}Cd (and for ^{181}Ta [4 - 6]) measured in the various phases of BaTiO₃ are listed in Table 1. In the case of the ^{111}Cd probes, one notes symmetric EFG's in the phases II and IV ($\eta_{\text{IV}} = \eta_{\text{II}} = 0$), while the EFG of the phase

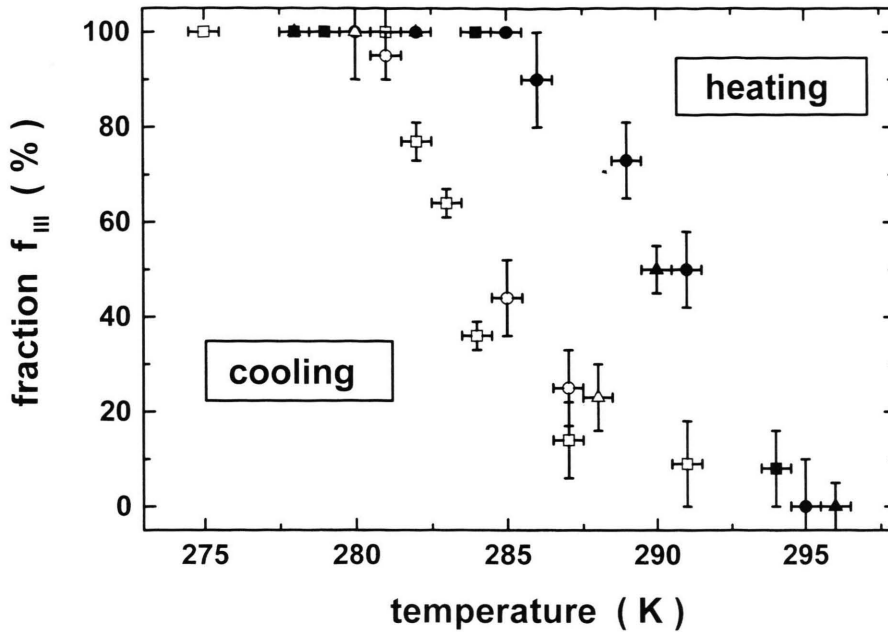


Fig. 2. Hysteresis of fraction III when heating (dots) or cooling (open squares) the sample across the III \rightarrow II phase transition.

Table 1. Electric field gradients of ^{111}Cd and ^{181}Ta probes in BaTiO₃.

Phase	— ^{111}Cd —			— ^{181}Ta [4 - 6] —		
	T (K)	ν_Q (MHz)	η	δ (MHz)	T (K)	ν_Q (MHz)
IV, rhomboh.	80	6.3(24)	0	3.1(16)	80	63(17)
III, orthorh.	227	22.0(8)	0.37(6)	1.1(6)	220	137(12)
II, tetrag.	293	33.3(7)	0	1.4(5)	293	205(12)
I, cubic	475	0	0	43(10)	400	0

III is asymmetric, $\eta_{\text{III}} = 0.37(6)$. All EFG's are well defined, with the width parameters being only $\delta = 1 - 3$ MHz. When comparing the EFG parameters for ^{111}Cd and ^{181}Ta probes, we note that the asymmetry parameters η agree fairly well for the various phases. Furthermore, the ratios of the quadrupole frequencies ν_Q for both probes agree with the ratio $\nu_Q(^{181}\text{Ta})/\nu_Q(^{111}\text{Cd}) = 6.5(10)$ predicted by the point charge model for the B-site, if we infer the appropriate quadrupole moments and Sternheimer factors of the two probe nuclei. This agreement of asymmetry parameters and frequency ratios thus strongly supports that both types of probe ions are being implanted into the B-site and substitute Ti. This conclusion is supported by PAC measurements with $^{181}\text{Hf}/^{181}\text{Ta}$ probes in SrHfO₃ and BaHfO₃ perovskites, following

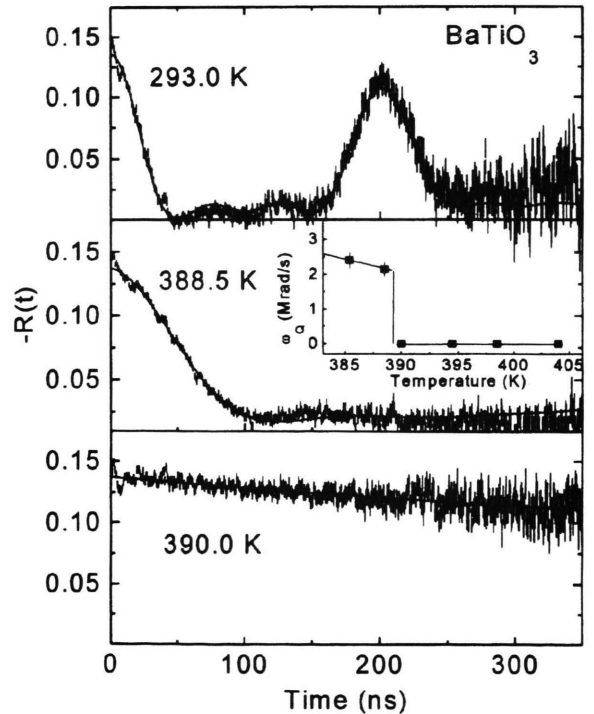


Fig. 3. Perturbation functions for ^{111}Cd in BaTiO₃ as observed near the II \rightarrow I phase transition. The inset shows the temperature dependence of the quadrupole frequency ω .

neutron activation of ¹⁸⁰Hf [9], and in our previous paper on ¹¹¹In/¹¹¹Cd in BaTiO₃ [8]. Similar results have also been discussed by Luthin *et al.* [13] for ¹¹¹Cd in ZrO₂ and HfO₂ and by Wiarda *et al.* [14] for a large number of other binary oxides.

4. Phase Transition Parameters

Let us now discuss, for the three phase transitions in BaTiO₃ considered, the temperature dependence of the fractions $f^{\uparrow/\downarrow}$ that reveal the hysteresis. As usual, we introduce the transition temperatures T_0^{\uparrow} and T_0^{\downarrow} , at which the two competing fractions are equal when increasing or decreasing the temperature across a phase transition. The quantity $\delta T_0 \equiv |T_0^{\uparrow} - T_0^{\downarrow}|$ measures the width of the hysteresis. The “smoothness” of a phase transition can be expressed by the quantities ΔT^{\uparrow} and ΔT^{\downarrow} , where we used the approximation

$$f^{\uparrow/\downarrow}(T) = \{1 \pm \exp[(T - T_0^{\uparrow/\downarrow})/\Delta T^{\uparrow/\downarrow}]\}^{-1}$$

for that fraction which has disappeared well *above* the transition temperature $T_0^{\uparrow/\downarrow}$. In Table 2, the deduced transition parameters are compared with the values reported from neutron diffraction, electric susceptibility and polarization experiments [1, 15, 16]. Only in the case of the III \rightarrow II transitions have we been able to obtain precise values of $T_0^{\uparrow/\downarrow}$ and $\Delta T^{\uparrow/\downarrow} = 1.7(2)$ K.

We first notice that the widths parameter δT_0 generally decreases for increasing transition temperatures, i. e. $\delta T_0^{\text{IV} \rightarrow \text{III}} \approx 7.5 - 25$ K, $\delta T_0^{\text{III} \rightarrow \text{II}} = 6$ K, and $\delta T_0^{\text{II} \rightarrow \text{I}} < 2$ K. Furthermore, the transition temperatures $T_0^{\uparrow/\downarrow}$ themselves measured with different methods do not

Table 2. Transition parameters in BaTiO₃ as obtained with different methods.

Transition	T_0^{\uparrow} (K)	T_0^{\downarrow} (K)	δT_0 (K)	Method	Ref.
IV \rightarrow III	202.5	195	7.5	PAC, ¹¹¹ Cd	Present work
	203	178	25	Polarization	
	195	178	17	Susceptibility	
III \rightarrow II*	290.4(2)	284.3(3)	6.1(3)	PAC, ¹¹¹ Cd	Present work
	274	269	5	PAC, ¹⁸¹ Ta	
	284	278	6	Neutron diff.	
	276	270	6	Polarization	
	277	270	7	Susceptibility	
II \rightarrow I	389	< 2	< 2	PAC, ¹¹¹ Cd	Present work

* $\Delta T^{\uparrow} = 1.6(2)$ K; $\Delta T^{\downarrow} = 1.8(3)$ K.

agree with each other. A possible explanation has been given by Zhong *et al.* [17] who found that the annealing conditions of the samples determine the grain size and consequently the transition parameters. In this way, changes of $T_0^{\uparrow/\downarrow}$ by as much as 10 K have been observed, if the annealing temperature varies between 1273 K and 1423 K.

In conclusion, we have determined the electric field gradients of dilute ¹¹¹Cd impurities in polycrystalline BaTiO₃ samples. For each of the known phase transitions, we have deduced the EFG parameters, the transition temperatures $T_0^{\uparrow/\downarrow}$ and, in the case of the orthorhombic \leftrightarrow tetragonal (III \leftrightarrow II) transition, the average smoothness parameter $\Delta T^{\uparrow/\downarrow} = 1.7(2)$ K. In view of the different values of $T_0^{\uparrow/\downarrow}$ observed with various methods, PAC measurements in single-crystals are required in future experiments. Furthermore, the influence of an external electric field on the EFG parameters also appears to be an interesting extension of the present study.

- [1] T. Mitsui *et al.*, Ferro- and Antiferroelectric Substances, Landolt-Börnstein, Group III, edited by K.-H. Hellwege; Springer-Verlag, Berlin 1969, Vol. 3.; M. E. Lines and A. M. Glass, Principles and Applications of Ferroelectrics and Related Materials, Clarendon-Press, Oxford 1979.
- [2] Y. Xu, Ferroelectric Mat. and their Applications, North-Holland, Amsterdam 1991.
- [3] D. Damjanovic, Rep. Progr. Phys. **61**, 1267 (1998).
- [4] G. L. Catchen, S. J. Wukitch, E. M. Saylor, W. Huebner, and M. Blaskiewicz, Ferroelectrics **117**, 175 (1991).
- [5] G. L. Catchen, E. F. Hollinger, J. M. Adams, and R. L. Rasera, Ferroelectrics **156**, 239 (1994).
- [6] G. L. Catchen, E. F. Hollinger, and T. M. Rearick, Z. Naturforsch. **51a**, 411 (1996).
- [7] G. Schäfer, P. Herzog, and B. Wolbek, Z. Phys. **257**, 336 (1972).
- [8] M. Uhrmacher, V. V. Krishnamurthy, K. P. Lieb, A. López-García, and M. Neubauer, Z. Phys. Chem. **206**, 249 (1998).
- [9] P. de la Presa, doctoral thesis, La Plata, Argentina (1997) unpubl.; P. de la Presa, R. E. Alonso, A. Ayala, S. Habenicht, V. V. Krishnamurthy, K. P. Lieb, A. López-García, M. Neubauer, and M. Uhrmacher, J. Phys. Chem. Solids **60**, 749 (1999).
- [10] I. J. Baumvol, A. Vasquez, J. Martinez, and F. C. Zawislak, Phys. Stat. Sol. **B79**, K65 (1977); P. de la

- [10] Presa, and A. López-García, *Rad. Eff. Def. Solids* **140**, 141 (1997).
- [11] M. Uhrmacher, K. Pampus, F. J. Bergmeister, D. Purschke, and K. P. Lieb, *Nucl. Instr. Meth.* **B9**, 234 (1985); M. Uhrmacher, M. Neubauer, W. Bolse, L. Ziegeler, and K. P. Lieb, *Nucl. Instr. Meth.* **B139**, 306 (1998).
- [12] G. Schatz and A. Weidinger, in *Nuclear Solid State Physics*, Wiley & Sons, New York 1996.
- [13] J. Luthin, K. P. Lieb, B. Lindgren, M. Neubauer, and M. Uhrmacher, *Phys. Rev.* **B57**, 15 272 (1998).
- [14] D. Wiarda, M. Uhrmacher, A. Bartos, and K. P. Lieb, *J. Phys.: Cond. Matter* **5**, 4114 (1993).
- [15] W. Merz, *Phys. Rev.* **76**, 1221 (1949).
- [16] H. H. Weider, *Phys. Rev.* **99**, 1161 (1955).
- [17] W. Zhong, P. Zhang, Y. Wang, and T. Ren, *Ferroelectrics* **160**, 55 (1994).